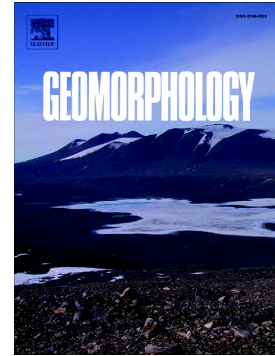


Accepted Manuscript

The establishment and influence of Baimakou paleo-dam in an upstream reach of the Yangtze River, southeastern margin of the Tibetan Plateau

Weiming Liu, Kaiheng Hu, Paul A. Carling, Zhongping Lai, Ting Cheng, Yali Xu



PII: S0169-555X(18)30326-X
DOI: doi:[10.1016/j.geomorph.2018.08.028](https://doi.org/10.1016/j.geomorph.2018.08.028)
Reference: GEOMOR 6491
To appear in: *Geomorphology*
Received date: 7 June 2018
Revised date: 18 August 2018
Accepted date: 21 August 2018

Please cite this article as: Weiming Liu, Kaiheng Hu, Paul A. Carling, Zhongping Lai, Ting Cheng, Yali Xu , The establishment and influence of Baimakou paleo-dam in an upstream reach of the Yangtze River, southeastern margin of the Tibetan Plateau. *Geomor* (2018), doi:[10.1016/j.geomorph.2018.08.028](https://doi.org/10.1016/j.geomorph.2018.08.028)

This is a PDF file of an unedited manuscript that has been accepted for publication. As a service to our customers we are providing this early version of the manuscript. The manuscript will undergo copyediting, typesetting, and review of the resulting proof before it is published in its final form. Please note that during the production process errors may be discovered which could affect the content, and all legal disclaimers that apply to the journal pertain.

**The establishment and influence of Baimakou paleo-dam in
an upstream reach of the Yangtze River, southeastern
margin of the Tibetan Plateau**

Weiming Liu^{1*}, Kaiheng Hu^{1*}, Paul A. Carling², Zhongping Lai³, Ting Cheng⁴, Yali Xu¹

¹ *Key Laboratory of Mountain Hazards and Surface Process, Institute of Mountain Hazards and Environment, Chinese Academy of Sciences, Chengdu 610041, China*

² *Geography & Environment, University of Southampton, Southampton, SO17 1BJ, UK*

³ *Institute of Marine Science, Shantou University, Shantou, 515063, China*⁴ *Ministry of Education Key Laboratory of Western China's Environmental Systems, College of Earth Environmental Sciences, Lanzhou University, Lanzhou 73000, China*

*Corresponding authors, E-mail address: liuwm@imde.ac.cn (W. Liu), khhu@imde.ac.cn (K. Hu).

Abstract: Landslide damming is an important disturbance factor in the river evolution of mountain belts and may control river morphology at variable timescales. This temporal aspect is mostly discussed in terms of the spatial relationships between the dams and river longitudinal profiles within any given region. Largely lacking are detailed studies of the geomorphic response for individual dams. Here we present field evidence and 24 optically stimulated luminescence (OSL) ages that show the history of a landslide dam in an upstream reach of Yangtze River at the southeastern margin of the Tibetan Plateau and its influence on river evolution. The distribution of lacustrine ages suggests that there was only one long-term damming event, induced by landslide blocking the river. The dammed lake formed at 12.1 ka, and disappeared at 7.5 ka. The estimated dam height was 120 m, lake area was 96 km², and lake volume was 7.5 km³. In addition, the grain size and distribution of lacustrine deposits indicate the dam failed cataclysmically when the lake finally drained. Today, the river long profile upstream of the dam site remains lower and the channel is wider in contrast to the downstream reach. Consequently, the former dam still influences channel morphology. Our study shows that the interaction of landslide dams with the rivers in the southeastern Tibetan Plateau may impeded valley incision and headward erosion in those cases where damming continued over periods of several thousand years.

Keywords: landslide dam, river long profile, luminescence dating, Yangtze River

1. Introduction

Although rivers occupy a relatively small area of the Earth's surface, rivers are a key force for controlling regional landform development (Whipple and Tucker, 1999; Whipple, 2004), and often river longitudinal profiles are used as the key indices for describing tectonics and surface processes (Kirby and Whipple, 2001; Clark *et al.*, 2004; Yang *et al.*, 2015). However, recent studies have suggested that natural dams have a proportionately larger role in controlling river evolution over timescales of 10^4 – 10^5 years in mountain terrains (Korup, 2006; Korup *et al.*, 2010; Walsh *et al.*, 2012; van Gorp *et al.*, 2016) in contrast to tectonics, climate, lithology, and regional base level changes. Consequently, it is important to understand the influence of dams, before changes in river channels can be used to infer the roles of other forcing factors.

Dams can affect the evolution of the river longitudinal profile in two contrasting manners. Dams can impede incision and produce local to regional knickpoints in the rivers longitudinal profiles. Previous studies argued that glacial and landslide damming of major rivers helped maintain plateau topography through impeding headward rivers incision into the Tibetan Plateau (Korup and Montgomery, 2008). Other studies also have found a correlation between knickpoints and dams on the rivers in the southeastern Tibetan Plateau (Ouimet *et al.*, 2007), the central Nepalese Himalayas (Walsh *et al.*, 2012), the New Zealand Southern Alps and the Swiss Alps (Korup, 2006) and the Tien Shan (Korup *et al.*, 2006). These studies indicate that damming prevents or reduces bed level degradation in the backwater reaches upstream of the dams. In contrast, when natural dam fail, dammed lakes can generate outburst floods, that will to incise through valley fill or bedrock, and promote valley erosion and headward incision. The results

from a study of the Sicachen glacial dam in the eastern Karakoram (Scherler *et al.*, 2014) and 17 landslide dams in eastern Oregon (Safran *et al.*, 2015) support the later effects. So, the effects of the dams on rivers still require additional investigation.

In previous studies, the focus mainly has been on the relationship between dams and the longitudinal profile of the rivers in specific regions to analyze the general geomorphic response (Ouimet *et al.*, 2007; Korup and Montgomery., 2008; Walsh *et al.*, 2012). There have been few studies of the geomorphic response of a river channel to the imposition of a single natural dam. Here we present the evidence for, and the optically stimulated luminescence (OSL) age of, one large paleo-landslide dammed lake - Baimakou - in an upstream reach of the Yangtze River at the eastern margin of the Tibetan Plateau (Figure 1). Further, we discuss the broader geomorphic effects of this dam.

2. Sampling and methods

2.1. Study area

The research area is located in the Sichuan-Yunan orogenic block, at the southeast margin of Tibetan Plateau (Zhang, 2013). Historically there have been many large earthquakes along this block boundary. The Luquan M6.1 earthquake occurred near the study area in 1985 (Wu *et al.*, 1990) (Figure 1). This area typically is a high elevation, low-relief landscape dissected by river gorges that are broadly distributed along the plateau margins (Clark *et al.*, 2006). The study area frequently experiences large landslides and the rivers are highly susceptible to landslide dams. Close to the study area, an historic landslide (1935) blocked the Yangzte River for three days, having formed a 50 m high dam, named the Luchedu dam (Li, 1996).

2.2. Geomorphic field work and sampling

To examine the evidence for and age of the dammed lake, we inspected several dozen cut banks distributed over more than 40 km along the Yangzte River and its tributary, the Longchuan River. We logged in detail 32 lacustrine sections, searching in particular for evidence of paleolakes. In the field, we measured the heights and thicknesses of 32 lacustrine deposits. We mapped the position, altitude, relative elevation to river levels using a laser TruPulse 200 range finder, and handheld Trimble Juno 3B GPS (global positioning system) devices with a real-time difference GPS system. The elevation is obtained using a hand-held GPS to record the latitude and longitude of site, which coordinates are input to the DEM of 1:50000 using ArcGIS 10.1 and the final accepted altitude read from the DEM.

After detailed fieldwork, seven lacustrine sections were selected to represent the lacustrine thickness for sampling for optically-stimulated luminescence (OSL) dating at well-spaced locations in the vertical. One hundred and thirty-one grain size samples were collected from the Najiu section to aid the interpretation of lake evolution.

2.3. OSL dating

The OSL samples were collected from cleaned profiles using steel pipes, ~4-cm in diameter and ~20 cm long, in homogeneous deposition characteristics within 30cm where possible. Twenty-four luminescence samples were collected. In the laboratory, extraction of quartz from samples and the OSL measurements, were performed in the red-light room. The outside part of the sample was first removed to measure water content and dose rate. Next, the residual samples were treated with 10% HCl for removal of carbonates, and then with 30% H₂O₂ for removal of organics, respectively. The remaining inorganic fractions were sieved to separate the dominant component of 38–63 μm , which were then treated with 35% H₂SiF₆ to remove feldspars. Then 10% HCl was used to remove fluorides (Lai, 2010). The remaining quartz grains were pasted with silicone oil onto the middle part (0.3 cm dia.) of 1-cm-diameter steel cups. OSL measurements were performed using an automated lexsyg research device model (Richter *et al.*, 2013), with an internal ⁹⁰Sr/⁹⁰Y beta flat source (0.120 Gy/s). Blue light-emitting diodes ($\lambda = 460 \pm 20$ nm) were applied to optical excitation for quartz grains. Luminescence signals were measured using a 9235QB photomultiplier (PMT) tube installed with Hoya U-340 filters.

The content of radio-elements (uranium (U), thorium (Th), and potassium (K)) was detected using the neutron activation method in the Chinese Atomic Energy Institute. Paleowater contents were estimated based on measured water content, paleo-process and modern average annual precipitation, using 15% with errors of $\pm 5\%$ for all samples as the paleomoisture content. The cosmic ray contribution was determined based on the burial depth and the geomagnetic coordinate of the research sites (Prescott and Hutton, 1994).

To determine the suitable preheat temperature, preheat plateau tests were carried out on BMKL1. D_e values of three aliquots were detected under each preheat temperature ranging from 180 °C to 300 °C with 20 °C uniform intervals. A preheat plateau of the D_e values between 220 and 260 °C was obtained (Figure 2A). Thus, the optical measurements were performed after heating at 260 °C for 10 s on natural (N) and regenerative doses, and cut-heat to 220 °C was used prior to test dose (TD). For 38–63 μm quartz, the α -value of 0.035 ± 0.003 was used for dose rate correction (Lai and Brückner, 2008).

Dose recovery and recycling ratio tests were carried out to check the reliability of the SAR protocol. We used BMKL1 for Dose recovery tests. The 48 Gy is used as natural D_e values for 24 aliquots from 180°C to 300 °C with 20 °C intervals. The ratios of the measured dose to an additional dose are between 0.9 and 1.1, proving the reliability of our OSL results (Figure 2B). Aliquots with a recycling ratio outside the range from 0.9 to 1.1 were not used.

2.4. Equivalent dose (D_e) determination

The combination of SAR and the standard growth curve (SGC) protocols has been applied successfully to date other lacustrine deposits (see summary in Lai *et al.*, 2014). Eight aliquots were first measured by the SAR method. Then, a SGC of each sample was established by average of those eight growth curves. To obtain a D_e , every value of L_N/T_N was matched in the SGC. The consistency of the SGC D_e values and the SAR D_e values (Table S1), suggests that the SGC method could be used for D_e determination. The final D_e was determined by the mean of all SAR D_e values and SGC D_e values.

2.5. Geomorphic analysis

To learn more about the effect of the landslide dam on the river channel, the channel width was measured using Google Earth images (date: November 26th, 2016) by calculating the width using the Thiessen Polygons method within the platform of ArcGIS 10.1. The channel width selected is the modern wetted-width calculated every kilometer over 300 km. We also extracted the river longitudinal profiles and calculated the channel slope using the 90 m SRTM (Shuttle Radar Topography Mission) digital elevation model. The elevation was extracted from every cell of the SRTM. The slope was calculated for every kilometer reach. In addition, the area and volume of the Baikou palaeo-dammed lake were also calculated using SRTM data.

3. Results

3.1. Lake sediments within the study areas

Lake sediments were found to be mainly laminated clay and silts (Figures S1-8), and the only bed of coarse pebbles was found within the Baimakou profile (Figure S1). All profiles lie on the Yangtze River and the Longchuan River, and there were no visible depositional hiatuses or unconformity contacts in any of the studied sections. These lacustrine deposits have the following characteristics. Firstly, all lacustrine deposits are distributed within a narrow strip along the valley margins on both sides of the Yangtze River (Figure 1). The distribution of 32 lacustrine sections (Table S2.) surveyed reflect the narrow lake morphology, and the altitude of every section is between 912-1030 m asl (Figure 3). Second, lacustrine sediment at each section tends to overlies pre-lake strata that differs from neighboring sections. This result indicates that there was no uniform geological substratum within the lake basin before the lake formed, which can be explained more clearly in Figure S1 ~S5. The lacustrine sediment of the Baimakou section overlies fluvial pebbles (Figure S1). The lake deposits of the Xincunliang section overlies metamorphic rocks (Figure S2). The Dawanzi section overlies red diamicton, that may be a debris flow deposit (Figure S3). The Najiu section overlies the red Yuanmou Formation, which is famous for being the formation within which the first specimen of *Homo erectus* was discovered (Hu, 1973) (Figure S4). Third, the tributary valleys on both sides of the river are also filled with lacustrine deposits (Figure S5). This phenomenon indicates that the formation of the valleys and the course of the river is earlier than that of the lacustrine deposits. These characteristics of the lacustrine deposition suggested it formed by a main valley damming event.

3.2. The characteristics of the Baimakou palaeo-landslide dam

The paleo-landslide named Baimakou landslide is delimited by a clear armchair-shaped geomorphic feature on the left bank (Figure 4), while residual landslide dam debris masses are distributed on both banks of the main valley. The lithology of the base rock for Baimakou landslide is purple red mudstone and sandstone. Using Google Earth, the highest altitude in the source area (scar in Figure 4) of the landslide is about 1390 m a.s.l. (above sea level), whilst the elevation of the river is 910 m a.s.l., such that the difference is 480 m. Moreover, the original area of the landslide dam is estimated to be approximately 3.24 km², whereas the areas of the remaining landslide dam debris masses on the left and right sides are calculated at about 1.20 and 1.23 km² respectively. The primary volume is about 0.34 km³ estimated using a relationship formula of volume and area scaling;

$$V = \alpha A^\gamma \quad (\text{Larsen } et al., 2010), \quad (1)$$

where V is the volume (m³), A is the area (m²), and α and γ are power-law scaling parameters; $\alpha=0.23$ and $\gamma=1.41$ were used (Larsen *et al.*, 2010).

3.3. OSL dating results

Figure 5A shows the representative OSL decay curves of YJTL6. The OSL signals decreased rapidly in the first second of stimulation, showing that the OSL signal was based by the fast component. Recuperate signal of all samples when there is no irradiation was below 1%. Figure 5B shows the growth curves and SGC for sample YJTL6. Taking YJTL6 as an example, its D_e values show a normal distribution and a tight symmetric peak, suggesting that the residual signals were generally fully bleached prior to deposition (Figure 5C). All eight growth curves were not saturated by 50 Gy and can be well fitted with the exponential plus linear equation. The OSL ages are shown in Figure 6 and are also listed in Table S1.

4. Discussion

4.1. The age and extent of Baimakou dammed lake

The 24 OSL dating results were all from within the age range of 7.0 ka to 14.8 ka (Figure 6 and Table S1). The OSL ages at the top of the Azhuhe, Mamula, and Najiu sections were relatively older than ages in the lower part of its section (Figure 6B, C and F). This apparent age inversion may be caused by the measuring error of the dose and the annual dose rate, because it can be overlapped to lower dating results in the range of the two times standard deviation. In addition, the other five samples near the top of the lacustrine deposit (within 5 m and 30% upperpart) were between 7.0-7.8 ka. The age of these three samples is relatively dispersed between 8.5~14.8 ka. Therefore, these three ages were not involved in determining the age of this lake. If the standard deviations are considered, the other OSL ages were all in stratigraphic order in sections, which allow us to have a strong confidence in the reliability of these remaining OSL ages.

Four dating results at the top (within the top 2 m) of four lacustrine sections (Baimakou, Mamula, Xincunliang, and Jiangtou) could be used to indicate the timing of the end of the dammed lake. The five ages were similar, ranging from 7.3 ± 0.8 to 7.8 ± 0.6 ka i.e. within the Holocene (Walker *et al.*, 2014). The middle age of five top ages (7.5 ka) was selected as representative of the date indicating the end age for the dammed lake. Except in the case of the Azhuhe section, the base of the lacustrine sediments was observed in the other six sections. Except for the age of 7.0 ± 0.5 ka at the base of the Mamula section (Figure 6C), the five other age determinations were within the range 10.1 ± 0.8 to 14.1 ± 0.8 ka. The middle age of five base ages (12.1 ka) was selected as representative of the date indicating the formation age of the dammed lake. In addition, within the lacustrine sediments, as noted above, there were no stratigraphic discontinuities or evident of erosional contacts found in any of surveyed sections. Consequently, it is concluded that the paleo-dammed lake formed at about 12.1 ka and sedimentation was more-or-less continuous until 7.5 ka; thus, the lake was sustained for several thousands of years.

Because no detailed analysis of the age and structure of the Baimakou landslide dam has yet been completed, it cannot be deduced why it lasted for several thousand years. Many factors, such as the landslide volume and material composition, as well as the rate of inflow to the dammed lake, would impact the longevity of a landslide dam (Costa and Schuster, 1988). Other landslide-dammed lakes, such as the Kalopani and Beshkiol rockslide dams, were also sustained for several thousand years (Korup *et al.*, 2006).

Landslides can be activated by a variety of factors including seismic activities, heavy precipitation, and river incision. In addition to triggering the large slope failure that formed the dam, usually, large earthquakes lead to slope instability over large areas of river catchments, potentially supplying coarse clastic materials to the river channel (Parker *et al.*, 2011). Thus, slope-derived clastic materials then can be transferred into the dammed lake rapidly (Li *et al.*, 2016). Therefore, coarse clastic sediment usually appears in abundance in the lower sections of the sediment fill of dammed lakes before the formation of clay or silt lacustrine sediments. Such examples occur in the many dammed lakes formed in 2008 (Wenchuan Mw 7.9 earthquake; Liu *et al.*, unpublished data) as well as within the Jintang dammed lake, also in the upper Yangtze River (Higgitt *et al.*, 2014). In contrast, the silt lacustrine deposits of the Baimakou dammed lake all directly overlie basal strata, while clastic sediment, deposited penecontemporaneously with the limnic sediments, was not found. Therefore, it is concluded that this dammed lake was not caused by an earthquake. Rather, paleoclimate studies show that rainfall in the eastern monsoon regions began to increase during the last deglaciation (at least 14.7 ka) (Chen *et al.*, 2015), earlier than the formation age of the dam impounding the Baimakou lake (12.1 ka). Therefore, increasing rainfall could have induced the Baimakou landslide by destabilizing hill slopes. However, during the last deglaciation, there was more melt water runoff from the many glaciers in the southeastern Tibetan Plateau (Fu *et al.*, 2013), increasing river monsoon or glacial-melt runoff should lead to rapid incision and formed T1 in the upstream of Yangtze River (Su *et al.*, 2013), that also would be

conducive to landsliding and landslide damming of rivers (Azañón *et al.*, 2005; Bilderback *et al.*, 2015). So, increasing rainfall and river incision in concert possibly induced the Baimakou landslide.

The lake deposits were all at elevations between 912 and 1030 m (Figure 3). The ages of all lacustrine profiles at comparable elevations were similar (Figure 6). Therefore, we suggested that there was only one stage of sedimentation within a single paleo-dammed lake at Baimakou on the Yangtze River. The elevation of the upper limit of the lake deposits (1030 m) was slightly lower than the maximum altitude of the paleo-landslide (1040 m) (Figure S9). Hence, using the lake surface elevation of 1030 m, the dam was 120 m high, the estimated lake area was 96 km², the volume was 7.5 km³, and the lake was 178 km in length.

The elevation of most lacustrine deposits was much lower than the elevation of lake surface (Figure 3). The ages at the top of most lacustrine sections are similar, indicating that most of the lacustrine sections are relatively well preserved and the lake was not filled completely by deposits. In addition, the grain size of the lacustrine deposition will gradually become coarser in the process of lake shallowing due to an increase in riverine and slope washed clastic sediments being concentrated within the topmost lake deposits. However, the grain size of Najiu section does not coarsen upwards (Figure 7). So, the elevation data and the grain size data of the lacustrine deposits all indicate that no shallowing processes occurred within this lake prior to its final draining. Rather the lake disappeared abruptly, suggesting an outburst flood happened with the lake drawing down rapidly when the dam failed. Using the average thickness (14 m) of 18 lacustrine profiles from our field measurements as the thickness of sediments in the all of the lake, the water volume when the lake outburst occurred was about 6.24 km^3 . the peak discharge (Q_p) of the break flood was approximately $8.2 \times 10^4 \text{ m}^3/\text{s}$, determined by the formula $Q_p = 0.3 (VD)^{0.46}$ (Cenderelli, 2000), V is water volume, D is water depth, $V = 6.24 \times 10^6 \text{ km}^3$ and $D = 106 \text{ m}$. That volume is more than the average flow ($3760 \text{ m}^3/\text{s}$) in the Longjie hydrological station, and also is greater than the largest modern flood ($3.2 \times 10^4 \text{ m}^3/\text{s}$) that was recorded at Longjie in 1924 (Luo, 2006).

4.2. Implications for the landslide damming influence on the evolution of upper Yangtze River

The thick and extensive lacustrine fill in upstream of Baimakou dam at the Yangtze River testifies to several thousand years of protracted upstream sediment deposition. Although the overall longitudinal profile slope change is frequent (Figure 8), we can still suggest that the impact of the dam is greater. Because, the slope value within 40 km upstream the dam site is only 0.5‰, and very small. The slope value within 20 km downstream the dam is very large, with 1.0‰. In addition, the widths of the channel within the former lake basin (i.e upstream of the dam) differ to the downstream widths (Figure 8A). The width behind the dam average 286 m, and below the dam the channel width average 223 m. This difference in width is due to the damming still having an effect on the modern channel, encouraging deposition of the river bed above the dam site and impeding erosion. Therefore, the river response to the Baimakou landslide is consistent with the results from the Yalong River and Dadu River - also at the southeastern margin of the Tibetan Plateau (Ouimet *et al.*, 2007) where the presence of a dam inhibited river bed erosion upstream of the impoundment. Previous study also reveals similar results in the Himalaya Range, in New Zealand, in the Tianshan Mountains and within the Alps (Korup, 2006; Korup *et al.*, 2006, 2010). However, in the case of 17 landslide dams in Oregon State (United States of America), only four landslide dams elevate the river longitudinal profile (Safran *et al.*, 2015) possibly due to the short-time persistence of most of the landslides.

Numerical modal studies have been used to suggest whether or not large landslide dams have noticeable effects on river erosion, depending on the duration of individual dams and their temporal and spatial distribution (Ouimet *et al.*, 2007; van Gorp *et al.*, 2014). After 7.5 kyr, the geomorphic response of the river to the landslide dam also can be seen today from the measurements obtained within this study. There were many other dammed lacustrine deposits distributed on the upstream of Yangtze River (Xu, 2011; Chen *et al.*, 2013; Wang *et al.*, 2014). Although further research is needed on other dams, it is possible to speculate that these dams have a similar effect on the river evolution as with the Baimakou dam. We suggest that the frequent pre-historic and historic damming plays a significant role in the incision and deposition along the upstream course of the Yangtze River, thus mediating the modern river bed slopes and channel widths.

5. Conclusions

We present evidence that the Baimakou paleo-landslide formed a lake that persisted for several thousand years. The 24 OSL ages from seven lacustrine sections indicate that a single paleo-lake formed around 12.1 ka, but had disappeared by 7.5 ka. The estimated lake area was 96 km² with an altitude of 1030 m, and the volume of the impoundment was 7.5 km³ before sedimentation reduced this initial volume. It could be inferred from the stratigraphy within the lake sediments that a river incision-induced landslide was the main cause of this damming. After several thousand years of stability, the Baimakou landslide dam ultimately failed catastrophically, and formed a flood with a maximum discharge of around 8.2×10^4 m³/s. The dam location still leads to a wider modern channel immediately upstream of the former dam and the longitudinal river profile slope in the vicinity of the lake remains reduced despite the dam failing some 7.5 ka ago.

Acknowledgments

We thank Zhengfeng Zhu and Cheng Chen for fieldwork assistance, Yinzhen Xia and Huai Su for help in the laboratory. This research was supported by National Key Basic Research Program of China (2015CB452704), the National Natural Science Foundation of China (41661144028 and 41771023), and Self-support Project (SDS-QN-1602) and the 135 Strategic Program (SDS-135-1701) from the Institute of Mountain Hazards and Environment, CAS.

References

Azañón, J.M., Azor, A., Pérez-Peña, J.V., Carrillo, J.M., 2005. Late Quaternary large-scale rotational slides induced by river incision: The Arroyo de Gor area (Guadix

- basin, SE Spain). *Geomorphology* 69, 152-168.
- Bilderback, E.L., Pettinga, J.R., Litchfield, N.J., Quigley, M., Marden, M., Roering, J.J., Palmer, A.S., 2015. Hillslope response to climate-modulated river incision in the Waipaoa catchment, East Coast North Island, New Zealand. *Geol. Soc. Am. Bull.* 127, 131-148.
- Cenderelli, D.A., 2000. Floods from Natural and Artificial Dam Failures, In: Wohl, E.E. (Ed.), *Inland Flood Hazards: Human, Riparian, and Aquatic Communities*. Cambridge University Press, Cambridge pp, 73-103.
- Chen, F., Xu, Q., Chen, J., Birks, H.J.B., Liu, J., Zhang, S., Jin, L., An, C., Telford, R.J., Cao, X., Wang, Z., Zhang, X., Selvaraj, K., Lu, H., Li, Y., Zheng, Z., Wang, H., Zhou, A., Dong, G., Zhang, J., Huang, X., Bloemendal, J., Rao, Z., 2015. East Asian summer monsoon precipitation variability since the last deglaciation. *Sci. Rep.* 5, 11186, doi: 10.1038/srep11186.
- Chen, J., Dai, F., Lv, T., Cui, Z., 2013. Holocene landslide-dammed lake deposits in the Upper Jinsha River, SE Tibetan Plateau and their ages. *Quat. Int.* 298, 107-113.
- Clark, M.K., Royden, L.H., Whipple, K.X., Burchfiel, B.C., Zhang, X., Tang, W., 2006. Use of a regional, relict landscape to measure vertical deformation of the eastern Tibetan Plateau. *J. Geophys. Res.* 111, F03002, doi: 10.1029/2005JF000294.
- Clark, M.K., Schoenbohm, L.M., Royden, L.H., Whipple, K.X., Burchfiel, B.C., Zhang, X., Tang, W., Wang, E., Chen, L., 2004. Surface uplift, tectonics, and erosion of eastern Tibet from large-scale drainage patterns. *Tectonics*, 23, TC1006,

doi:10.1029/2002TC001402.

Costa, J.E., Schuster, R.L., 1988. The formation and failure of natural dams. *Geol. Soc. Am. Bull.* 100, 1054-1068.

Fu, P., Stroeven, A.P., Harbo, r J.M., Hättestrand, C., Heyman, J., Caffee, M.W., Zhou, L.,. 2013. Paleoglaciation of Shaluli Shan, southeastern Tibetan Plateau. *Quat. Sci. Rev.* 64, 121-135.

Higgitt, D., Zhang, X., Liu, W., Tang, Q., He, X., Ferrant, S., 2014. Giant palaeo-landslide dammed the Yangtze river. *Geoscience Letters* 1, 6.

Hu, C., 1973. Ape-man teeth from Yuanmou, Yunnan. *Acta Geological Sinica* 65-71(in Chinese with English abstract).

Kirby, E., Whipple, K., 2001. Quantifying differential rock-uplift rates via stream profile analysis. *Geology* 29, 415-418.

Korup, O., 2006. Rock-slope failure and the river long profile. *Geology* 34, 45-48.

Korup, O., Montgomery, D.R., 2008. Tibetan plateau river incision inhibited by glacial stabilization of the Tsangpo gorge. *Nature* 455, 786-789.

Korup, O., Montgomery, D.R., Hewitt, K., 2010. Glacier and landslide feedbacks to topographic relief in the Himalayan syntaxes. *Proc. Nat. Acad. Sci. U.S.A.* 107, 5317-5322.

Korup, O., Strom, A.L., Weidinger, J.T., 2006. Fluvial response to large rock-slope failures: Examples from the Himalayas, the Tien shan, and the southern Alps in new Zealand. *Geomorphology* 78, 3-21.

Lai, Z., 2010. Chronology and the upper dating limit for loess samples from

- Luochuan section in the Chinese Loess Plateau using quartz OSL SAR protocol. *J. Asian Earth Sci.* 37, 176-185.
- Lai, Z.P., Mischke, S., Madsen, D., 2014. Paleoenvironmental implications of new OSL dates on the formation of the "Shell Bar" in the Qaidam Basin, northeastern Qinghai-Tibetan Plateau. *J. Paleolimnol.* 51, 197-210.
- Lai, Z.P., Zöller, L., Fuchs, M., Brückner, H., 2008. Alpha efficiency determination for OSL of quartz extracted from Chinese loess. *Radiat. Meas.* 43, 767-770.
- Larsen, I.J., Montgomery, D.R., Korup, O., 2010. Landslide erosion controlled by hillslope material. *Nature Geosci.*, 3, 247-251.
- Li, G., West, A.J., Densmore, A.L., Hammond, D.E., Jin, Z., Zhang, F., Wang, J., Hilton, R.G., 2016. Connectivity of earthquake-triggered landslides with the fluvial network: Implications for landslide sediment transport after the 2008 Wenchuan earthquake. *J. Geophys. Res.* 121, 703-724.
- Li, T., 1996. Landslide hazard mapping and management in China. International Centre for Integrated Mountain Development, Kathmandu, Nepal.
- Luo, C. 2006. The collection of Investigated Historical Flood in China (in chinese). Cathay Bookshop, Beijing.
- Ouimet, W.B., Whipple, K.X., Royden, L.H., Sun, Z., Chen, Z., 2007. The influence of large landslides on river incision in a transient landscape: Eastern margin of the Tibetan Plateau (Sichuan, China). *Geol. Soc. Am. Bull.*, 119, 1462-1476.
- Parker, R.N., Densmore, A.L., Rosser, N.J., de Michele, M., Li, Y., Huang, R., Whadcoat, S., Petley, D.N., 2011. Mass wasting triggered by the 2008 Wenchuan

- earthquake is greater than orogenic growth. *Nature Geosci.* 4, 449-452.
- Prescott, J.R., Hutton, J.T., 1994. Cosmic ray contributions to dose rates for luminescence and ESR dating: Large depths and long-term time variations. *Radiat. Meas.* 23, 497-500.
- Richter, D., Richter, A., Dornich, K., 2013. Lexsyg — A new system for luminescence research. *Geochronometria* 40, 220-228.
- Safran, E.B., O'Connor, J.E., Ely, L.L., House, P.K., Grant, G., Harrity, K., Croall, K., Jones, E., 2015. Plugs or flood-makers? The unstable landslide dams of eastern Oregon. *Geomorphology* 248, 237-251.
- Scherler D, Munack H, Mey J, Eugster P, Wittmann H, Codilean AT, Strecker MR. 2014. Ice dams, outburst floods, and glacial incision at the western margin of the Tibetan Plateau: A >100 k.y. chronology from the Shyok Valley, Karakoram. *Geol. Soc. Am. Bull* **126**: 738-758.
- Su H., Ming Q., Pan B., Gao H., Zhang W., Dong M., 2013. The Analysis Discussions on the Chronological Frame of Jinshajiang River Valley-drainage. *Journal of Mountain Science*, 685-692. (in Chinese with English abstract)
- van Gorp, W., Schoorl, J.M., Temme, A.J.A.M., Reimann, T., Wijbrans, J.R., Maddy, D., Demir, T., Veldkamp, T., 2016. Catchment response to lava damming: integrating field observation, geochronology and landscape evolution modelling. *Earth Surf. Proc. Land.* 41, 1629-1644.
- van Gorp, W., Temme, A.J.A.M., Baartman, J.E.M., Schoorl, J.M., 2014. Landscape Evolution Modelling of naturally dammed rivers. *Earth Surf. Proc. Land.* 39,

1587-1600.

- Walker, M.J.C., Gibbard, P.L., Berkelhammer, M., Bjorck, S., Cwynar, L.C., Fisher, D.A., Long, A.J., Lowe, J.J., Newnham, R.M., Rasmussen, S.O., Weiss, H., 2014. Formal Subdivision of the Holocene Series/Epoch, In: Rocha, R., Pais, J., Kullberg, J.C., Finney, S. (Eds.), STRATI 2013: First International Congress on Stratigraphy At the Cutting Edge of Stratigraphy. Springer International Publishing, Cham pp, 983-987.
- Walsh, L.S., Martin, A.J., Ojha, T.P., Fedenczuk, T., 2012. Correlations of fluvial knickzones with landslide dams, lithologic contacts, and faults in the southwestern Annapurna Range, central Nepalese Himalaya. *J. Geophys. Res.*, 117, F01012, doi:10.1029/2011JF001984.
- Wang, P., Chen, J., Dai, F., Long, W., Xu, C., Sun, J., Cui, Z., 2014. Chronology of relict lake deposits around the Suwalong paleolandslide in the upper Jinsha River, SE Tibetan Plateau: Implications to Holocene tectonic perturbations. *Geomorphology* 217, 193-203.
- Whipple, K.X., 2004. Bedrock Rivers and the Geomorphology of Active Orogens. *Annu. Rev. Earth Planet. Sci.* 32, 151-185.
- Whipple, K.X., Tucker, G.E., 1999. Dynamics of the stream-power river incision model: Implications for height limits of mountain ranges, landscape response timescales, and research needs. *J. Geophys. Res.*, 104, 17661-17674.
- Wu, M., Wang, M., Sun, C., Ke, Z., Wang, P., Chen, Y., 1990. Accurate hypocenter determination of aftershocks of the 1985 Luquan earthquake. *Acta Seism. Sin.*,

12, 121-129.

Xu, Z., 2011. Deposits of Zhaizicun landslide dammed lake along Jinsha River and its implication for the genesis of Xigeda formation. *Geological review* 57, 675-686 (in Chinese with English abstract).

Yang, R., Willett, S.D., Goren, L., 2015. In situ low-relief landscape formation as a result of river network disruption. *Nature* 520, 526-529.

Zhang, P.Z., 2013. A review on active tectonics and deep crustal processes of the Western Sichuan region, eastern margin of the Tibetan Plateau. *Tectonophysics* 584, 7-22.

Figure Captions

Figure 1. Study area in the southeastern of Tibetan Plateau. (A) Overview of Tibetan Plateau. (B) Map of the southeastern of Tibetan Plateau with the OSL dating locations. Other lacustrine sections found in the field are marked as black boxes. Historical earthquakes, historical damming event and major faults are also shown in this figure.

Figure 2. (A) Results of preheat plateau test for sample BMKL 1. The grey bar indicates preheat plateau observed from 220 to 260 °C, the error bars indicate the standard error of three aliquots. (B) Results of dose recovery test for BMKL 1. The error bars indicate the standard error of three aliquots.

Figure 3. River Longitudinal profile showing present-day elevation (black line is Yangtze River; gray line is Longchuan River), the top of all surveyed sections are shown by black triangles.

Figure 4. Characteristics of Baimakou paleolandslide. (A) Google earth image (from November 20th 2017) of landslide area (www.google.com/earth). (B) The Baimakou landslide scar from the right bank of Yangze River.

Figure 5. Typical OSL decay curves (A), growth curves (B) of 8 cups and equivalent dose (D_e) distributions (C).. (A) 0 and 73.4 Gy are regenerate signals, TD is test signal, N is natural signal. (B) The growth curves are using exponential add linear fitting. The equation of average growth curve is $y = 12.4(1 - \exp(-0.136x)) - 0.022x + 0.02$.

Figure 6. Plan view image of the sampling area shown in Figure 1 together with summary sedimentary sections and the luminescence dating results of the sections investigated.

Figure 7. The change of grain size of the Najiu section from bottom to top. (A) Proportion of grain size curve greater than 63microns in size. (B) Md is median grain size.

Figure 8. River slope and channel width of Yangze river in the study region.

Figure 1.

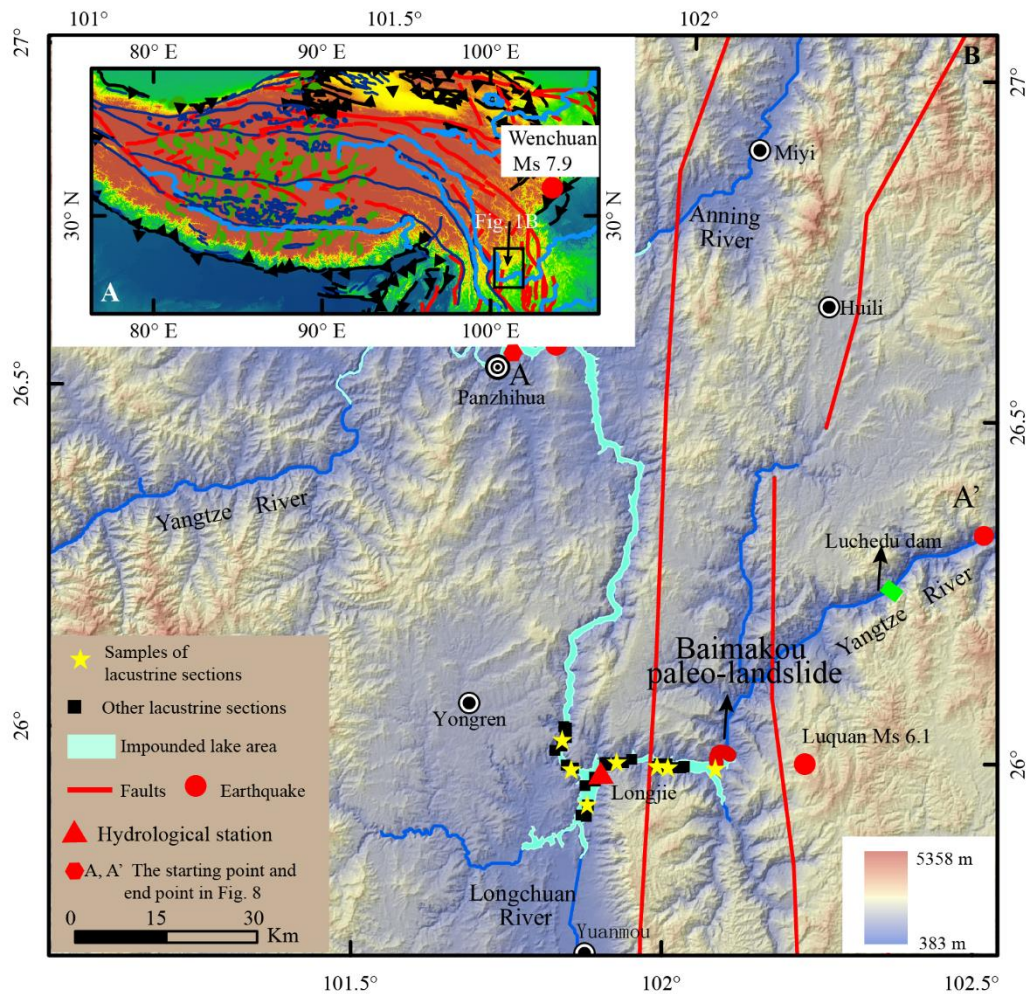


Figure 2.

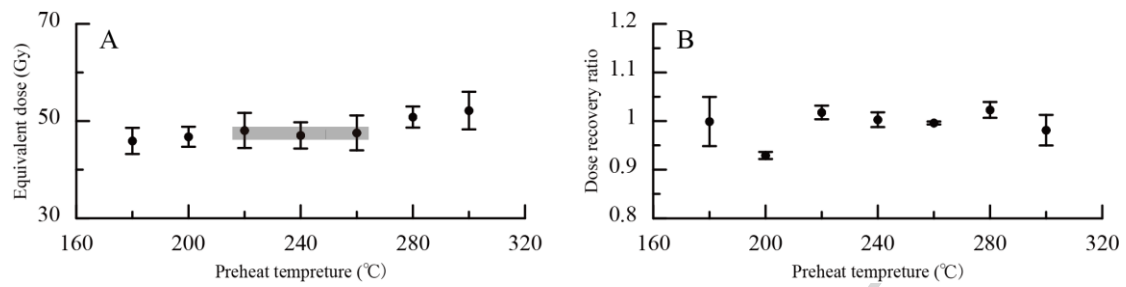


Figure 3.

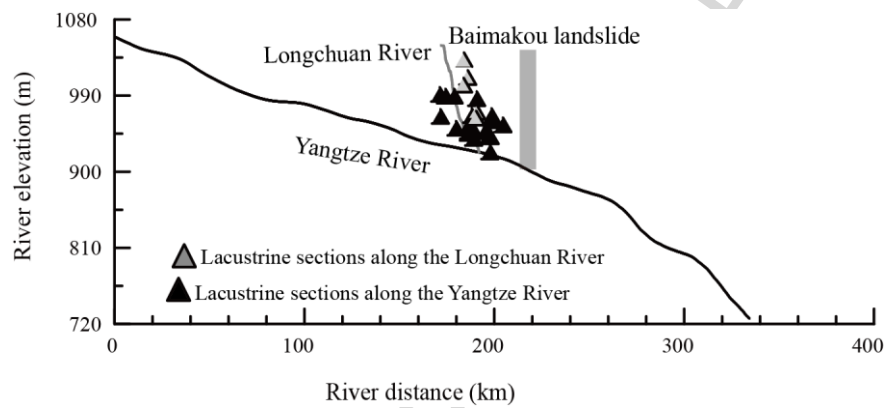


Figure 4.

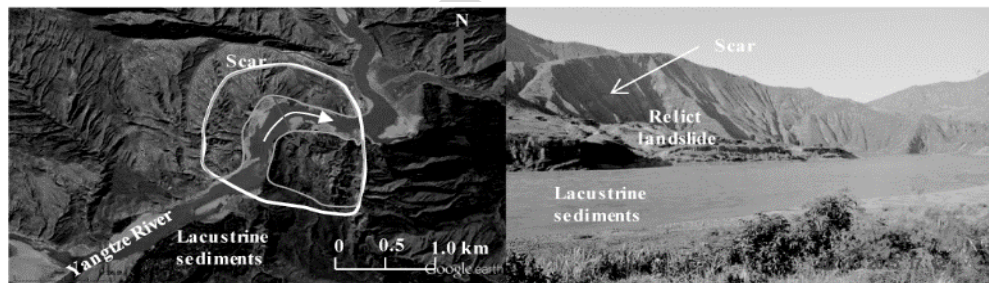


Figure 5.

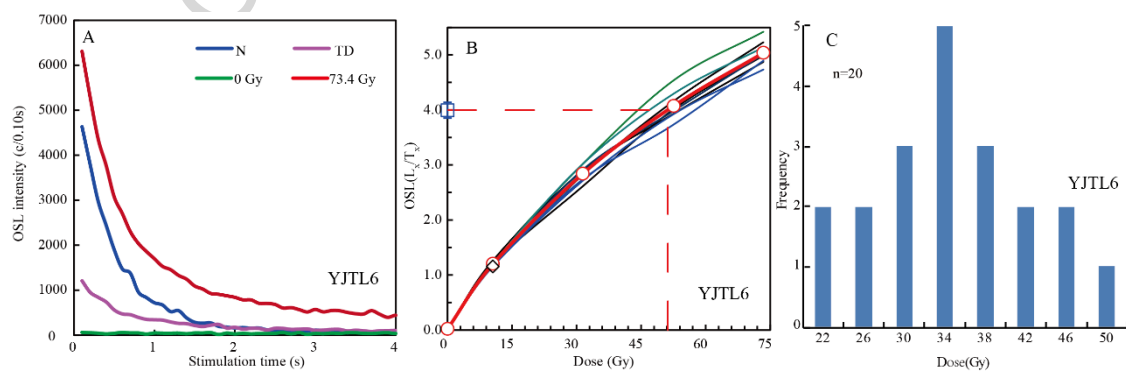


Figure 6.

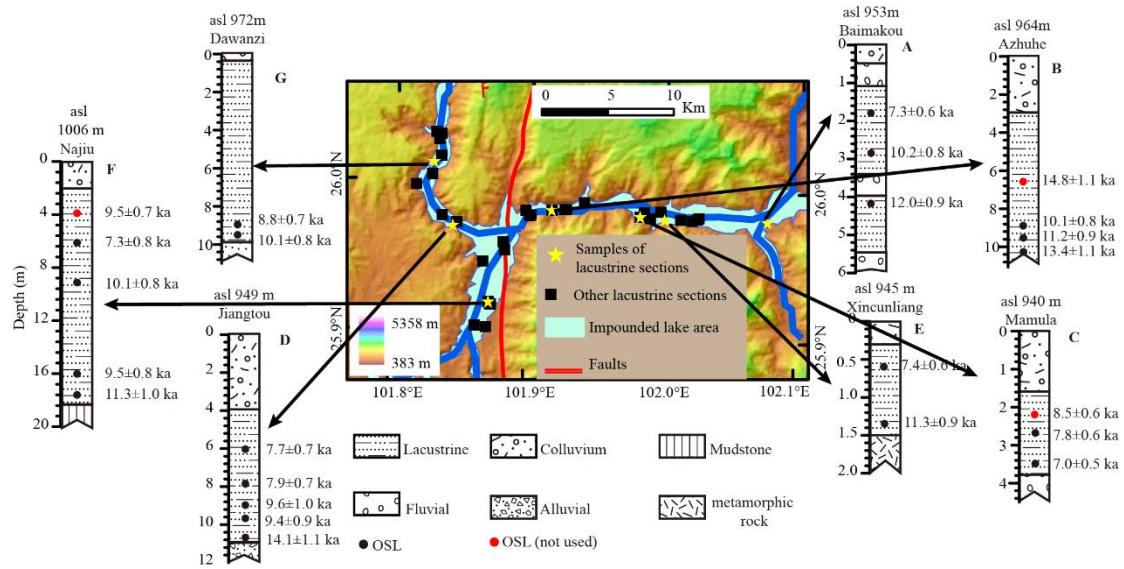


Figure 7.

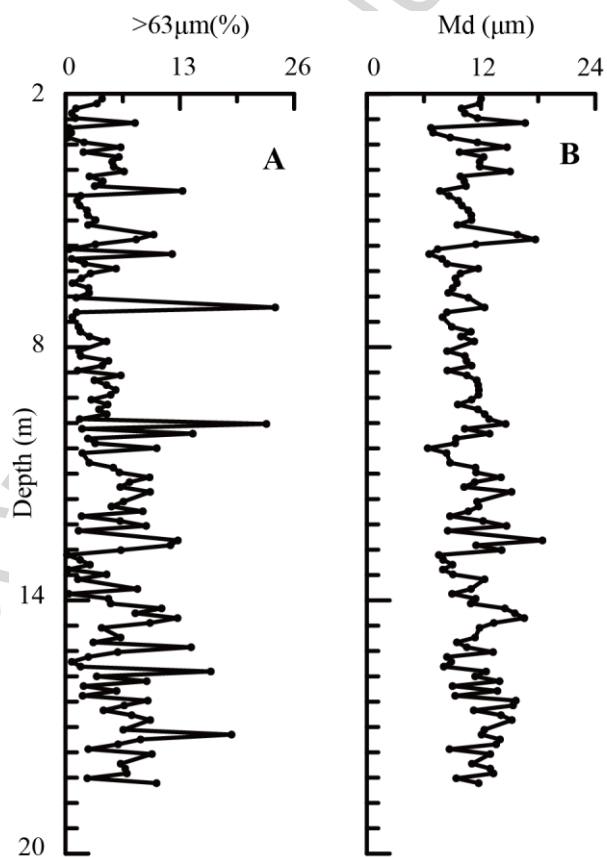
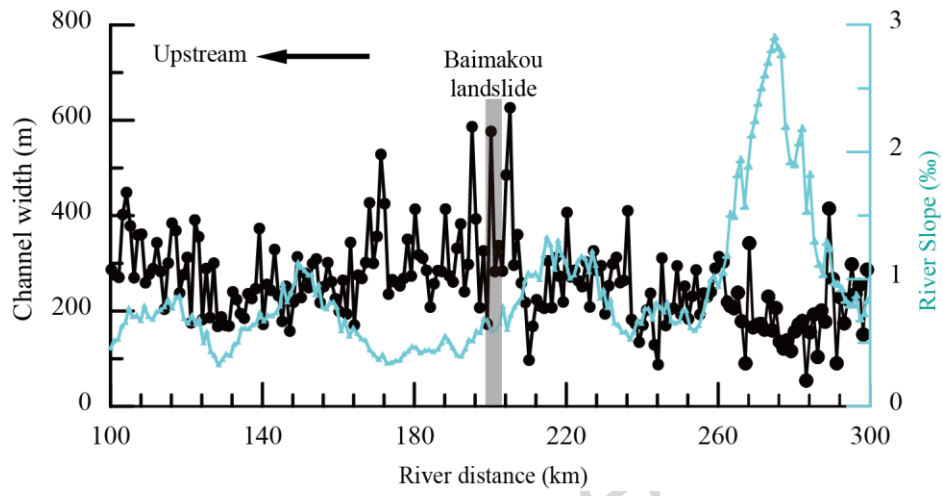


Figure 8.



Highlights:

- 1 The 24 ages show the Baimakou dammed lake continued from 12.1 ka to 7.5 ka.
- 2 It was not likely to be induced by earthquake from the lacustrine characteristics.
- 3 The grain size and distribution of deposits indicated the dam failed cataclysmically.
- 4 The dams continued few thousand years may impede valley and headward erosion.

ACCEPTED MANUSCRIPT